

# Dalton Transactions

An international journal of inorganic chemistry

Accepted Manuscript

This article can be cited before page numbers have been issued, to do this please use: Y. Zheng, P. Datta, D. Bowers, M. Kurokawa, H. Wang, Z. Yue, H. Xiao, S. Bang, M. Stilgenbauer and T. Beach, *Dalton Trans.*, 2020, DOI: 10.1039/D0DT01297A.



This is an Accepted Manuscript, which has been through the Royal Society of Chemistry peer review process and has been accepted for publication.

Accepted Manuscripts are published online shortly after acceptance, before technical editing, formatting and proof reading. Using this free service, authors can make their results available to the community, in citable form, before we publish the edited article. We will replace this Accepted Manuscript with the edited and formatted Advance Article as soon as it is available.

You can find more information about Accepted Manuscripts in the [Information for Authors](#).

Please note that technical editing may introduce minor changes to the text and/or graphics, which may alter content. The journal's standard [Terms & Conditions](#) and the [Ethical guidelines](#) still apply. In no event shall the Royal Society of Chemistry be held responsible for any errors or omissions in this Accepted Manuscript or any consequences arising from the use of any information it contains.

## Engineering Liposomal Nanoparticles of Cholesterol-Tethered Amphiphilic Pt(IV) Prodrugs with Prolonged Circulation Time in Blood

Received 00th January 20xx,  
Accepted 00th January 20xx

DOI: 10.1039/x0xx00000x

www.rsc.org/

Payel Datta,<sup>a</sup> Scott Bang,<sup>b</sup> Zhizhou Yue,<sup>a</sup> Travis Beach,<sup>a</sup> Morgan Stilgenbauer,<sup>a</sup> Han Wang,<sup>a</sup> David J. Bowers,<sup>a</sup> Manabu Kurokawa,<sup>b</sup> Haihua Xiao,<sup>c</sup> and Yao-Rong Zheng<sup>\*a</sup>

Cisplatin is a platinum-based chemotherapeutic agent widely used in the treatment of various solid tumors. However, a major challenge in the use of cisplatin and in the development of cisplatin derivatives, namely Pt(IV) prodrugs, is their premature reduction in the bloodstream before reaching cancer cells. To circumvent this problem, we designed liposomal nanoparticles coupled with a cholesterol-tethered amphiphilic Pt(IV) prodrug. The addition of cholesterol served to stabilize the formation of the liposome, while selectively incorporating cholesterol as the axial ligand also allowed the Pt(IV) prodrug to readily migrate into the liposomal bilayer. Notably, upon embedding into the nanoparticles, the Pt(IV) prodrug showed marked resistance against premature reduction in human plasma *in vitro*. Pharmacokinetic analysis in a mouse model also showed that the nanoparticles significantly extend the half-life of the Pt(IV) prodrug to 180 min, which represents a > 6-fold increase compared to cisplatin. Importantly, such lipid modification did not compromise the genotoxicity of cisplatin, as the Pt(IV) prodrug induced DNA damage and apoptosis in ovarian cancer cell lines efficiently. Taken together, our strategy provides a novel insight as to how to stabilize a platinum-based compound to increase the circulation time *in vivo*, which is expected to enhance the efficacy of drug treatment.

### Introduction

Cisplatin, an FDA-approved platinum-based chemotherapy drug, is commonly used to treat a wide range of solid tumors.<sup>1, 2</sup> The anticancer activity of cisplatin is attributed to its ability to form intra- and interstrand cross-links with DNA via coordination to purine nucleotides.<sup>1, 3, 4</sup> The cross-links inhibit DNA and RNA polymerases, therefore leading to cell death via apoptosis. Only a small portion of the administered cisplatin reaches cancer cells, due to its poor pharmacokinetics and deactivation via coordination to off-target nucleophiles, e.g. human serum albumin and glutathione.

Pt(IV) prodrugs are emerging as a promising replacement for current platinum based drugs.<sup>5-21</sup> Oxidation of the square-planar cisplatin gives the kinetically inert pseudo-octahedral Pt(IV) prodrug with two additional "axial" ligands. Within the reducing environment of cancer cells, the Pt(IV) center is

converted to Pt(II) via the release of two ligands, regenerating cisplatin in the process.<sup>22</sup> Careful selection of the axial ligands allows for the modification of the physical, chemical, and biological properties of the Pt(IV) prodrugs, allowing for the design of more efficient medicines. For example, lipophilic axial ligands have been used to improve the rate of cell entry for platinum compounds.<sup>23-26</sup> Recently, a number of reports show that a secondary anticancer agent can be incorporated as an axial ligand to generate a "dual-threat" Pt(IV) prodrug, which is more potent against cancer cells than cisplatin.<sup>27-31</sup> Importantly, axial ligands can facilitate the nanodelivery of platinum therapeutics.<sup>32-35, 21, 36, 37</sup> Lipophilic carboxylate ligands allow for encapsulation of Pt(IV) prodrugs in polymeric nanoparticles, carbon nanotubes, and gold nanoparticles. For example, Yang and coworkers have demonstrated that conjugation of Pt(IV) prodrugs with cholesterol facilitates nanodelivery using polymeric nanoparticles.<sup>20</sup> This would reduce reduction of the prodrug in the bloodstream, currently a major challenge in developing Pt(IV) prodrugs.<sup>38-40</sup>

In this study, we engineered a cholesterol-tethered amphiphilic Pt(IV) prodrug (**1**) to facilitate nanodelivery using liposomal nanoparticles (LNs), thereby stabilizing the Pt(IV) prodrug. By incorporating cholesterol as an axial ligand, we can readily insert the Pt(IV) prodrug into the liposomal bilayer. This lets the Pt(IV) prodrug resist premature reduction in human plasma, and has shown to achieve a long circulation time in the mouse model.

<sup>a</sup> Department of Chemistry and Biochemistry, Kent State University, 236 Integrated Sciences Building, Kent, Ohio 44242.

<sup>b</sup> Department of Biological Sciences, Kent State University, 211 Cunningham Hall, Kent, Ohio 44242.

<sup>c</sup> Beijing National Laboratory for Molecular Sciences, State Key Laboratory of Polymer Physics and Chemistry, Institute of Chemistry, Chinese Academy of Sciences, Beijing 100190, P. R. China.

Email: yzheng7@kent.edu

Electronic Supplementary Information (ESI) available: Characterization of the cholesterol-tethered Pt(IV) prodrug (**1**), formulation of the liposomal nanoparticles (LNs), and cellular uptake and RT-PCR analysis of LNs and cisplatin in A2780cis cells. See DOI: 10.1039/x0xx00000x.

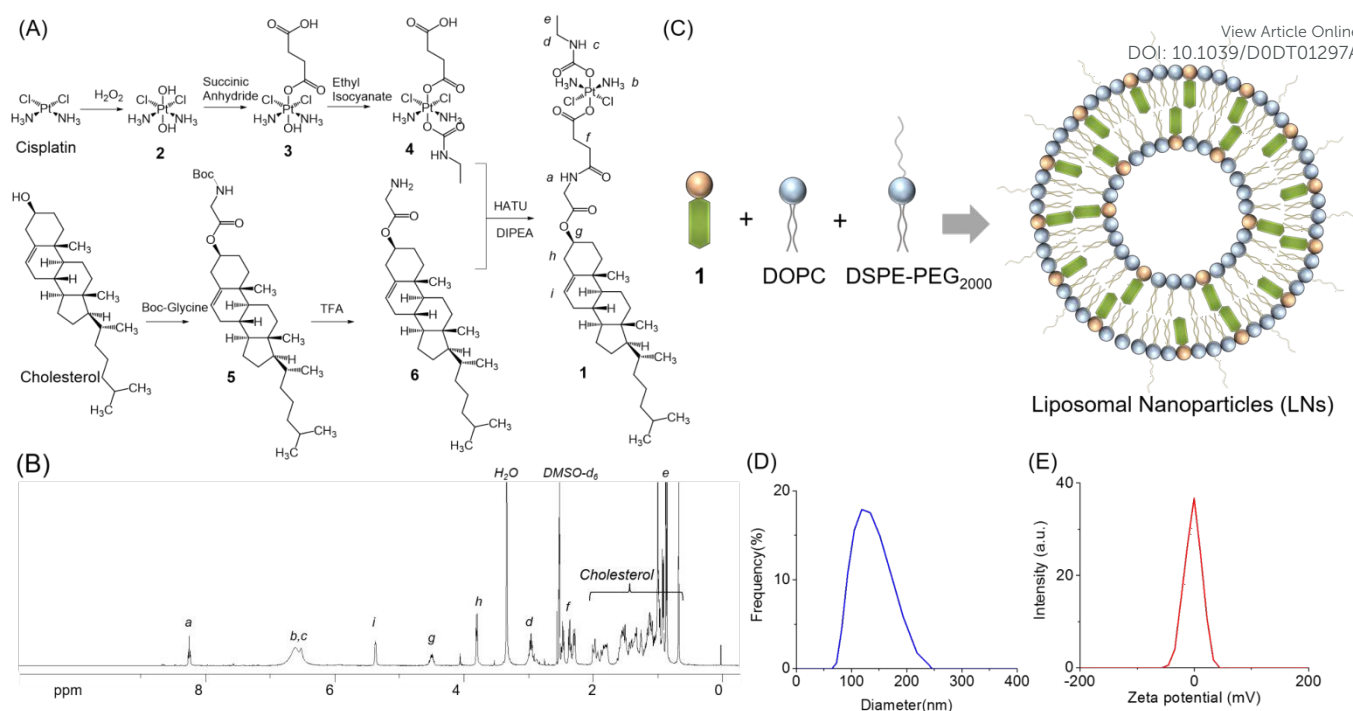


**Figure 1.** Formulation of the liposomal nanoparticles (LNs) of the cholesterol-tethered Pt(IV) prodrug (**1**), DOPC, and DSPE-PEG<sub>2000</sub>: (A) Synthesis of the cholesterol-tethered Pt(IV) prodrug (**1**); (B) <sup>1</sup>H NMR spectrum of **1** in DMSO-d<sub>6</sub>; (C). Graphical representation of the self-assembly of LNs; (D) DLS analysis of LNs in PBS; (E). Zeta-potential of LNs in PBS.

## Results and discussion

**Synthesis and characterization of the cholesterol-tethered amphiphilic Pt(IV) prodrug (**1**).** Synthesis of the Pt(IV) prodrug (**1**) is depicted in Fig 1A. Briefly, cisplatin was oxidized to oxoplatin (**2**) using hydrogen peroxide. Succinate anhydride further reacted with **2** to form the asymmetrical Pt(IV) compound (**3**). Ethyl isocyanate subsequently reacted with the Pt-bound hydroxide ligand to afford **4**. The glycine-conjugated cholesterol (**6**) was conjugated to the Pt(IV) center by the HATU-catalyzed amide bond formation reaction between **4** and **6**. The overall yield was 40%. The cholesterol-tethered Pt(IV) compound (**1**) was characterized by <sup>1</sup>H and <sup>13</sup>C NMR spectroscopy, electrospray ionization mass spectrometry (ESI-MS), and HPLC. In the <sup>1</sup>H NMR spectrum (Fig 1B), the broad signal at 6.510 ppm corresponds to the amine groups of the Pt(IV) center. The signals at 2.94 ppm and 0.975 ppm is the ethyl group attaching to the carbamate. The singlet at 3.32 ppm is attributed to the CH<sub>2</sub> within the glycine residue. In ESI-MS spectrum (Fig S1 in Supporting Information), the isotopically resolved signal at *m/z* = 930.3876 agrees with the theoretical value of **1** (*m/z* = 930.3869). HPLC analysis of the final product indicated that the purity of compound **1** from the described synthetic method was 95%.

### Self-assembly of LNs of the cholesterol-tethered Pt(IV) prodrug (**1**).

As shown in Fig 1C, the Pt(IV) compound (**1**) self-assembles with 1,2-dioleoyl-*sn*-glycero-3-phosphocholine (DOPC) and 1,2-distearoyl-*sn*-glycero-3-phosphoethanolamine-N-

(polyethylene glycol)-2000 (DSPE-PEG<sub>2000</sub>) to form liposomal nanoparticles (LNs) in aqueous solution. The assembly was optimized by varying the amounts of **1** as shown in Table S1 (see Supporting Information). The encapsulation efficiency ( $EE = w_{\text{encapsulated Pt}} / w_{\text{total Pt}}$ ) and loading capacity ( $LC = w_{\text{encapsulated Pt}} / w_{\text{total}}$ ) were determined using the results of GFAAS analysis. At the ratio of 2.5: 0.25: 2 (DOPC: DSPE-PEG<sub>2000</sub>: **1**), the liposomal formulation achieved optimized EE (66.1%) and LC (27.9%). According to the DLS data (Fig 1D), the overall size of LNs is approximately 101.6 nm. The zeta-potential was determined to be -3.20 mV (Fig 1E).

**Stability of LNs against ascorbic acid and human plasma.** Next, we assessed the stability of the Pt(IV) prodrug in LNs against ascorbic acid, a reducing agent commonly found in cells, using dialysis. In the experiment, drug releasing profiles of LNs were studied in PBS (pH = 7.4) with different conc. of ascorbic acid (0, 20 μM, and 20 mM) using micro-dialysis bags (3.5 kDa MWCO). In its intact form compound **1** stays on the bilayer of LNs, but upon reduction cisplatin is readily released from LNs. LNs show a very slow release of cisplatin in PBS with low conc. of ascorbic acid (0 and 20 μM), and less than 25% of the Pt species were released after 160 h (Fig 2A). At a high conc. of ascorbic acid (20 mM), payload release can reach 40%. The stability of the Pt(IV) prodrug (**1**) within LNs placed in human plasma was also investigated using size exclusion chromatography (SEC) and graphite furnace atomic absorption spectroscopy (GFAAS). Briefly, LNs were added to human plasma, and incubated at 37 °C for 24 hr. The plasma samples before and after incubation

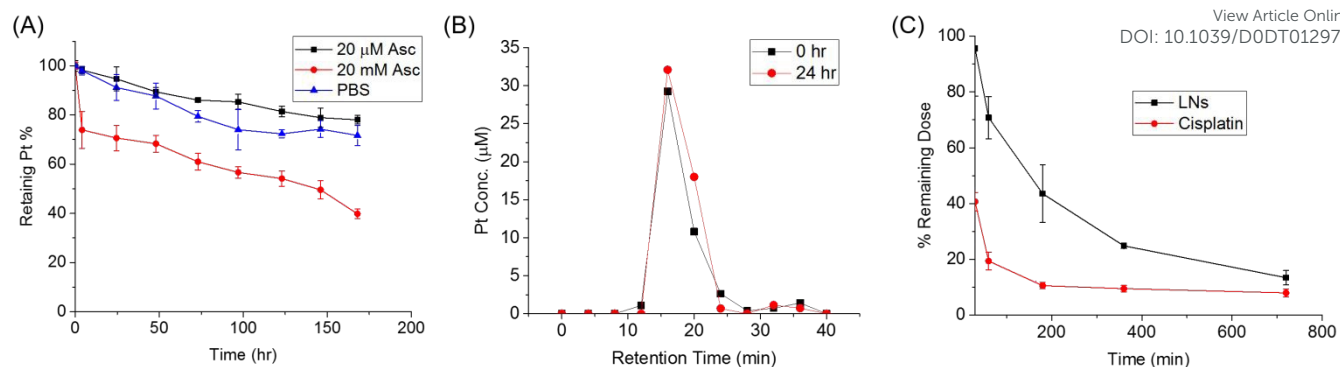


**Figure 2.** Assessments of the stability of LNs: (A) Release profiles of LNs against PBS, PBS with 20  $\mu\text{M}$  ascorbic acid (20  $\mu\text{M}$  Asc), and PBS with 20 mM ascorbic acid (20 mM Asc); (B) The SEC traces analyzed by GFAAS of LNs in human plasma before (0 hr) and after (24 hr) incubation at 37  $^{\circ}\text{C}$ ; (C). *In vivo* pharmacokinetic analysis shows that LNs extend the half-life of the prodrug to 180 min, which represents a > 6-fold increase compared to cisplatin in the same animal model (KM mice,  $n=3$ ).

were subjected to SEC analysis, with the Pt contents of the fractions obtained by SEC subjected to further analysis by GFAAS. As shown in Fig 2B, the SEC traces analyzed by GFAAS are similar with respect to the plasma samples before and after 24-hr incubation. To sum up, our data suggests that LNs are stable against plasma and they can be slowly reduced by high conc. of ascorbic acid.

**Assessment of the circulation time of LNs *in vivo*.** We further evaluated the pharmacokinetics of LNs in a mouse model. Both LNs and cisplatin (2 mg/kg) were injected into C57BL/6 mice. Blood samples were extracted from the mice periodically, and the Pt contents were then analysed using inductively coupled plasma mass spectrometry (ICP-MS). As shown in Fig 2C, LNs extend the half-life of the Pt(IV) prodrug (**1**) to 180 min, which represents a > 6-fold increase compared to cisplatin (< 30 min).

**Cytotoxicity profile.** The *in vitro* anticancer activity of LN loaded with **1** was assessed by using the MTT assay. Four human cancer cell lines, cisplatin-sensitive ovarian cancer cell line A2780, cisplatin-resistant ovarian cancer cell line A2780cis, breast cancer cell line MDA-MB-231, and the non-small cell lung cancer cell line A549 were evaluated. Cancer cells were treated with cisplatin or LNs for 72 h and cell viability was evaluated. Due to its poor solubility **1** was not included in the test.  $\text{IC}_{50}$  values, which represent the concentration required to inhibit growth by 50%, are given in Fig 3A. Across all the tested lines, LNs exhibit similar *in vitro* cytotoxicity to cisplatin.

**Cellular uptake.** An important factor in drug effectiveness is its ability to enter the cell. In order to determine the effect LNs have on drug uptake, GFAAS was used to study cell entry by analysing the intracellular Pt contents of cells exposed to Pt formulations. A2780cis cells were treated with LNs or cisplatin ([Pt] = 10  $\mu\text{M}$ ), then after 21 h, the cellular Pt contents were measured. The results (Fig S2) show that the cellular uptake of cisplatin was  $50.9 \pm 5.25$  pmol/million cells, while the uptake of LNs was approximately 7 times higher ( $351.33 \pm 45.01$  pmol/million

cells). This indicates that the LNs facilitate the cell entry of the payloads. However, due to the slow drug release profiles of LNs, only a small portion of cisplatin releases from the nanoparticles to kill cancer cells.

**Biomarker of DNA damage.** To confirm DNA damage caused by the release of cisplatin, we monitored changes in expression of biomarkers related to DNA damage pathways. A2780cis cells were incubated with cisplatin (8  $\mu\text{M}$ ) or LNs ([Pt] = 6  $\mu\text{M}$ ). As determined by flow cytometry (Fig 3B), the A2780cis cells treated with LNs show a marked increase in phosphorylated H2AX ( $\gamma\text{H2AX}$ ), a marker for DNA damage.<sup>41, 42</sup> To further assess DNA damage, we performed RT-PCR analysis for a panel of genes known to be induced following DNA damage (p21, PUMA, BAX, NOXA, and APO1).<sup>43</sup> We found that LNs induced expression of these genes similarly to cisplatin at 24 hr and 48 hr post treatment (Fig 3C and Fig S3). These results are consistent with the determined cytotoxicity profiles.

**Cellular responses.** Using a dual staining Annexin V/PI flow cytometry assay, the occurrence of apoptosis was investigated in A2780cis cells treated with LNs and cisplatin. The results in Fig 3D clearly indicate that LNs can efficiently induce apoptosis in A2780cis cells. LNs ([Pt] = 6  $\mu\text{M}$ ) prompt A2780cis cells to undergo early (7.04%) and late (1.92%) stage apoptosis after 72 h of incubation, the populations of which were similar to those of cisplatin.

## Conclusions

We have presented the development of liposomal nanoparticles to extend the circulation time of embedded Pt(IV) prodrugs *in vivo*. In this study, we demonstrated that the cholesterol-tethered amphiphilic Pt(IV) prodrug (**1**) can be formulated into liposomal nanoparticles. These liposomes resist degradation in ascorbic acid as well as human plasma. *In vivo* pharmacokinetic analysis shows that the liposomal nanoparticles extend the half-life (180 min) of the Pt(IV) prodrug to > 6-fold increase compared to cisplatin (< 30 min) in the mouse model. Furthermore, the lipid-modification did not

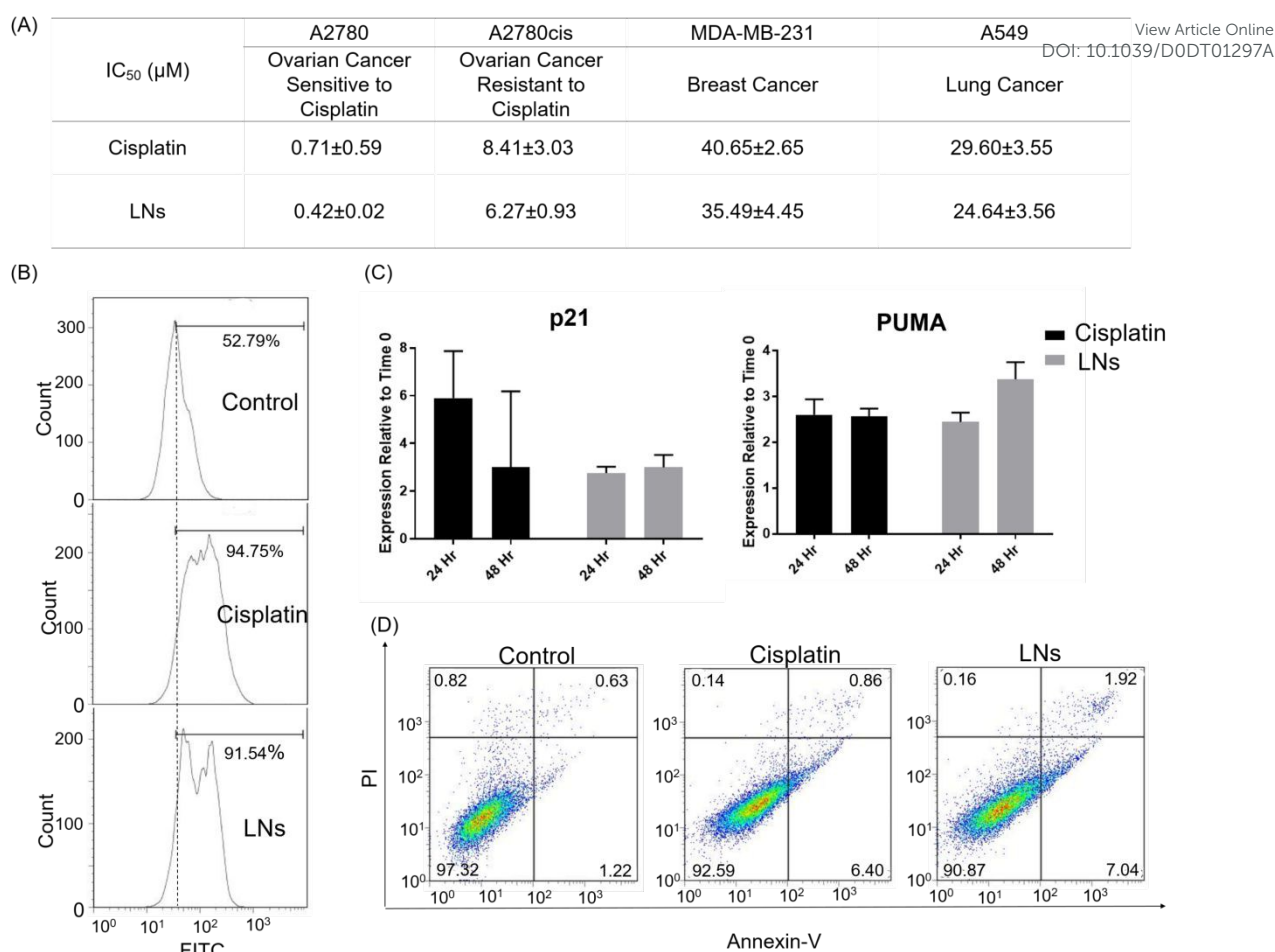


**Figure 3.** Cellular responses of LNPs: (A) Cytotoxicity profiles of cisplatin and LNPs against a panel of human cancer cell lines (72 h); (B) Flow cytometric analysis of phosphorylation of H2AX ( $\gamma$ H2AX) of A2780cis cells treated with cisplatin (8  $\mu$ M) and LNPs ([Pt] = 6  $\mu$ M) for 72 h; (C) mRNA levels of p21 and PUMA in A2780cis cells treated with cisplatin (8  $\mu$ M) or LNPs ([Pt] = 6  $\mu$ M); (D) Flow cytometric analysis of apoptotic events in A2780cis cells treated with cisplatin (8  $\mu$ M) and LNPs ([Pt] = 6  $\mu$ M) for 72 h.

compromise *in vitro* genotoxicity of the Pt(IV) prodrug, including the induction of DNA damage and apoptosis, compared to cisplatin. This study established a new platform for delivering amphiphilic Pt(IV) prodrugs. This new design would pave a new way toward controlled drug release to overcome drug resistance in ovarian cancer.

## Experimental

**General information.** Compound **2**, **3**, and **4** were prepared according to the reported literature.<sup>44, 45</sup> The chemical reagents used in this study were purchased from major chemical distributors, including Sigma Aldrich, Acros Organic, Alfa Aesar, TCI America, and Matrix Scientific. Human plasma was obtained from Innovative Research. A Bruker 400 NMR was used for NMR data acquisition (Frequency: 400 MHz for <sup>1</sup>H NMR; 100 MHz for <sup>13</sup>C NMR) and the plots were generated by TOPSPIN 3.2 software. For the NMR spectra, chemical shifts were given on the  $\delta$  scale (ppm) and were referenced to the residual solvent signals; Coupling constants *J* were reported in hertz (Hz). The abbreviations s, d, t, q and m were used for singlet, doublet,

triplet, quartet and multiplet, respectively. The high-resolution mass spectra of created ions were recorded on an Exactive Plus mass spectrometer (Thermo Scientific, Bremen, Germany). Mass spectra were recorded in the positive ionization mode with a scan range of 50–700 *m/z*, a mass resolving power setting of 140,000, and an automatic gain control (AGC) target value of  $1 \times 10^6$  ions. To ensure very high mass accuracy (found to be better than 1 ppm) the instrument was mass calibrated daily and a lock mass of *m/z* 371.10124, due to polysiloxane, was used throughout. Graphite furnace atomic absorption spectroscopic (GFAAS) measurements were taken on a PerkinElmer PinAAcle 900Z spectrometer.

**Synthesis of boc-glycine conjugated cholesterol (5).** Boc-glycine (2.63 g, 15 mmol), cholesterol (3.87 g, 10 mmol), DMAP (1.22 g, 10 mmol) were dissolved in dry DCM (100 mL) and cooled to 0 °C and stirred for 1 hr at 0 °C. This was followed by the addition of a DCM solution (50 mL) containing DCC (2.27 g, 11 mmol) over 15 min. This solution was stirred for 1 hr and brought to r.t. slowly, then further stirred for 66 hr at r.t. to give a white suspension. The suspension was filtered, washed with 5% citric

acid (25 mL, 4X) and brine, then dried over  $\text{Na}_2\text{SO}_4$ . The resultant product was purified by column chromatography using 100% DCM as eluent to give a white powder. Yield (2.45 g, 51%).  $^1\text{H}$  NMR (400 MHz,  $\text{CDCl}_3$ ):  $\delta$ : 5.368 (C=CHCH<sub>2</sub>, 1H, m), 4.965 (OCH, H, m), 3.869 (OCHCH<sub>2</sub>C, 2H, m), 2.336 (C=CHCH<sub>2</sub>, 2H, m); 1.495 (boc Hs), 0.670-2.398 (alicyclic protons from cholesterol).  $^{13}\text{C}$  NMR (100 MHz,  $\text{CDCl}_3$ ):  $\delta$ : 169.74, 155.67, 139.36, 122.92, 75.17, 56.67, 56.12, 50.00, 42.30, 39.71, 36.90, 36.55, 35.78, 31.89, 31.83, 28.32, 24.27, 23.82, 22.81, 21.02, 19.28, 18.70, 11.84. HR-MS (positive mode) for  $[\text{C}_{34}\text{H}_{58}\text{NO}_4]^+$ : m/z [M + H]<sup>+</sup> calc. 544.4362, obsd: 544.4360.

**Synthesis of glycine conjugated cholesterol (6).** Boc-glycine conjugated cholesterol (2.45 g, 4.5 mmol) was mixed with Trifluoroacetic acid (2.8 mL, 0.036 mol), dichloromethane (28 mL, 0.44 mol) and stirred at r.t. for 5 hr. The solvent was evaporated and dried under vacuum. The resultant solid was then treated with saturated  $\text{NaHCO}_3$  and extracted with DCM. The separated layer was washed with brine and dried over  $\text{Na}_2\text{SO}_4$ , concentrated, then dried under vacuum overnight. Yield (1.94 g, 97%).  $^1\text{H}$  NMR (400 MHz,  $\text{CDCl}_3$ ):  $\delta$ : 5.381 (C=CHCH<sub>2</sub>, 1H, m), 4.44 (OCH, H, m), 3.423 (OCHCH<sub>2</sub>C, 2H, m), 2.314 (C=CHCH<sub>2</sub>, 2H, m); 0.674-2.398 (alicyclic protons from cholesterol).  $^{13}\text{C}$  NMR (100 MHz,  $\text{CDCl}_3$ ):  $\delta$  = 173.62, 139.47, 122.83, 74.62, 56.68, 44.18, 42.30, 39.51, 38.11, 36.57, 35.78, 31.89, 31.84, 28.21, 24.27, 22.81, 21.02, 19.29, 18.71, 11.85. HR-MS (positive mode) for  $[\text{C}_{29}\text{H}_{50}\text{NO}_2]^+$ : m/z [M + H]<sup>+</sup> calc. 444.3836, obsd: 444.3836.

**Synthesis of cholesterol conjugated Pt(IV) prodrug (1).** **4** (75 mg, 0.15 mmol), HATU and DMF were stirred for 1 hr at r.t. followed by the addition of **6** (80 mg, 0.18 mmol) and stirred for 1 hr at r.t.. DIPEA (40  $\mu\text{L}$ ) was added to the mixture and stirred for 17 hr. The resultant yellow suspension was centrifuged, concentrated under reduced pressure, then brine solution was added to precipitate out the solid from the solution. The resultant solid was washed with water (2 mL, 2x) and lyophilized overnight to give a yellow solid. Further purification was completed by column chromatography using 5% methanol in DCM as the eluent. Yield (55 mg, 39 %).  $^1\text{H}$  NMR (400 MHz,  $\text{DMSO}-d_6$ ):  $\delta$ : 8.23 (1H, s, glycine CONH); 6.51 ( $\text{NH}_3$  and  $\text{NH}$  carbamate), 5.35 (C=CHCH<sub>2</sub>, 1H, m), 4.965 (OCH, 1H, m), 3.77 (OCHCH<sub>2</sub>C, 2H, m), 2.94 (2H, t, J=6.4 Hz,  $\text{CH}_2$  attached to carbamate); 2.43-2.32 (succinic  $\text{CH}_2$ , 4H, m); 2.26-0.65 (alicyclic protons from cholesterol, ethyl proton attached to carbamate).  $^{13}\text{C}$  NMR (100 MHz,  $\text{DMSO}-d_6$ ):  $\delta$  = 174.164, 172.405, 172.018, 169.829, 139.845, 139.827, 122.684, 74.325, 56.587, 5.042, 49.885, 42.321, 40.906, 40.330, 36.907, 36.539, 36.126, 35.659, 31.826, 31.789, 24.321, 23.658, 23.131, 22.861, 21.019, 19.420, 19.018, 12.385. HR-MS (positive mode) for  $[\text{C}_{36}\text{H}_{65}\text{Cl}_2\text{N}_4\text{O}_7\text{Pt}]^+$ : m/z calc: 930.3869, obsd: 930.3876.

**Self-assembly of LNs.** DOPC (2.5 mg), DSPE-PEG<sub>2000</sub> (0.25 mg), **1** (0.5, 1, 2, 3, 4 mg), and 1 mL chloroform were stirred in a 5 mL glass vial at r.t. for 5 min. The solvent was then evaporated under reduced pressure and the LNs were dried overnight in a

desiccator. LNs were then dissolved in 2 mL PBS, sonicated for 1 hr and filtered through 0.2  $\mu\text{m}$  filter before use in studies.

**Dialysis experiment** 1 mL of PBS solution (pH = 7.4) containing Liposome ([Pt] = 50  $\mu\text{M}$ ) was sealed in micro-dialysis bags (3 kDa MWCO) against 500 mL PBS or ascorbic acid solutions (20  $\mu\text{M}$  or 20 mM) at R.T. A series of samples were collected within the bags for every few hours and analysed with GFAAS. All measurements were done in triplicate.

**Stability in human plasma** LNs was added to 1-mL human plasma to reach [Pt] = 250  $\mu\text{M}$ . The plasma samples were subjected to SEC analysis before and after 24-hr incubation at 37 °C. The fractions collected from SEC at different time points were analysed using GFAAS.<sup>44, 45</sup>

**Cell line and cell culture** The human ovarian carcinoma A2780 and cisplatin resistant A2780cis cell lines were obtained from Sigma Aldrich, ovarian cancer cell line SKOV-3 was obtained from ATCC. Unless otherwise specified, cells were incubated at 37 °C in 5%  $\text{CO}_2$  and grown in RPMI 1640 with L-glutamine (Corning, Corning, NY, USA) for A2780 and A2780CP70 or DMEM 1 g/L glucose, with L-glutamine & sodium pyruvate (Corning, NY, USA) for A549 and MDA-MB-231 supplemented with 10% fetal bovine serum (FBS) and 1% penicillin/streptomycin. All cell lines were cultured at 37°C under an atmosphere containing 5%  $\text{CO}_2$ . Cells were passaged upon reaching 70-80% confluence by trypsinization and split in a 1:5 ratio.

**MTT assays** Cell viability was determined using the MTT assay. Cells were seeded in 96-well plates in 100- $\mu\text{L}$  solution per well to begin and were incubated for 24 hr at 37 °C, 5%  $\text{CO}_2$ . The following day, 1:4 serially diluted platinum drug-containing medium was added in 50  $\mu\text{L}$  portions across 6 sample groups. The cells were then incubated for 72 hr at 37 °C, 5%  $\text{CO}_2$ . Afterwards, 30  $\mu\text{L}$  of 3-(4,5-dimethylthiazol-2-yl)-2,5-diphenyltetrazolium bromide (MTT) (Alfa Aesar, Haverhill, MA, USA) (0.2 mg/mL) was added to each well. Cells were then incubated an additional 2-4 hr at 37 °C, 5%  $\text{CO}_2$ . The wells were then aspirated, followed by the addition of 200  $\mu\text{L}$  DMSO to each well. The plates were then shaken for 10min. Next, the plates were analysed for absorbance at 562nm with an ELx800 absorbance reader (BioTek, Winooski, VT, USA). Data was then analysed using Origin software to produce dose response curves and to determine  $\text{IC}_{50}$  values. All the measurements were done in triplicate.

**Cellular uptake evaluated by GFAAS** One million A2780cis cells were seeded on 6 well plate and incubated at 37 °C overnight. These cells were treated with cisplatin ([Pt] = 10  $\mu\text{M}$ ) or liposome ([Pt] = 10  $\mu\text{M}$ ) for 21 h at 37 °C. The remaining live cells were harvested by trypsinization and digested in 200  $\mu\text{L}$  65%  $\text{HNO}_3$  at r.t. overnight. The platinum content in the cells was analysed by GFAAS. All experiments were performed in triplicate.

**Flow cytometric analysis of  $\gamma$ H2AX** A2780cis cells were seeded in a 6-well plate at a concentration of  $2 \times 10^5$  cells/well. Cells were then incubated at  $37^\circ\text{C}$ , 5%  $\text{CO}_2$  for 24 hr. Next, liposome or cisplatin was added according to the  $\text{IC}_{50}$  determined from cell viability assay and incubated for 72 hr. Live cells were collected and 250  $\mu\text{L}$  BD Permeabilization solution was added to re-suspend the cells, which were then incubated for 20 min at  $4^\circ\text{C}$ . Cell pellets were collected, washed twice with 1X BD Perm/Wash buffer, and resuspended in 50  $\mu\text{L}$  of buffer. Alexa 488-anti  $\gamma$ H2AX antibody solution was then added and the samples were incubated in the dark for 60 min at r.t.. The final cell pellets were suspended in 200  $\mu\text{L}$  of PBS with 0.5% BSA and analysed by FITC channel on a FACSAria™II flow cytometer (BD Biosciences, Franklin Lakes, NJ, USA).

**Flow cytometric analysis of apoptosis:** A2780cis cells were seeded in a 6-well plate at a concentration of  $2 \times 10^5$  cells/well. Cells were then incubated at  $37^\circ\text{C}$  5%  $\text{CO}_2$  for 24 hr. Next, liposome or cisplatin was added according to the  $\text{IC}_{50}$  values determined by the cell viability assay and incubated for 72 hr. Cells were collected, resuspended in 1mL PBS, and counted. 1X binding buffer from the FITC Annexin V Apoptosis Detection Kit 1 (BD Biosciences, Franklin Lakes, NJ, USA) was then added to reach a concentration of  $10^6$  cells/mL. 100  $\mu\text{L}$  cell solution was transferred to a fresh 2 mL Eppendorf tube and 5  $\mu\text{L}$  of both Annexin V-FITC and PI solutions were added to cells. Cells were incubated 15 min at r.t. in the dark and then brought to 400 $\mu\text{L}$  volume. Cells were then analysed with FITC and PE channels on a FACSAria™ II (BD Biosciences, Franklin Lakes, NJ, USA) and data was processed using FlowJo software.

**Quantitative RT-PCR** RNA was isolated using a PureLink RNA Mini Kit (Invitrogen). cDNA was synthesized using a qScript cDNA synthesis kit (Quanta). RT-qPCR was performed using iTaq Universal SYBR Green Supermix (Bio-Rad) on a CFX96 Real-Time PCR Detection System (Bio-Rad). Target gene mRNA levels were normalized to RPLP0 and were compared using the delta-delta Ct method. The following primer sequences were used to perform RT-qPCR for human cells. APAF1 (forward 5'-TGCGCTGCTCTGCCTTCT-3', reverse 5'-CCATGGGTAGCAGCTCCTTCT-3'), BAX (forward 5'-CGAGTGTCTCAAGCGCATC-3', reverse 5'-GCAAAGTAGAAAAGGGCGACAAC-3'), NOXA (forward 5'-AAGAAGGCGCGCAAGAAC-3', reverse 5'-TCCTGAGCAGAAGAGTTTGGT-3'), P21 (forward 5'-TGCCGAAGTCAGTTCCTTGT-3', reverse 5'-CATGGTCTGACGGACATC-3'), PUMA (forward 5'-GACCTCAACGCACAGTACGA-3', reverse 5'-CACCTAATTGGGCTCCATCT-3'), RPLP0 (forward 5'-GCAATGTTGCCAGTGTCTG-3', reverse 5'-GCCTTGACCTTTTCAGCAA-3').

#### **In vivo pharmacokinetic analysis**

This study was performed in strict accordance with the NIH guidelines for the care and use of laboratory animals (NIH Publication No. 85-23 Rev. 1985) and was approved by the Institute of Chemistry Chinese Academy of Sciences Ethics

Committee. KM mice were randomly divided into two groups (n=3) with an average body weight of 200 g. Cisplatin and Liposomal nanoparticles (LNs) were injected into mice via the tail vein at a dose of 3.5 mg Pt/g body weight. Subsequently, blood were collected into the EP tubes at various time points post injection including 0 h, 0.5 h, 1 h, 3 h, 6 h and 12h. Pt contents in serum were detected by ICP-MS after centrifugation.

#### **Conflicts of interest**

There are no conflicts to declare.

#### **Acknowledgements**

Y.-R. Z thanks the financial support provided by the startup fund, Farris Family Innovation Fellowship, and LaunchPad Award provided by Kent State University. M.K. is a recipient of the Mary Kay Foundation research grant.

#### **Notes and references**

1. D. Wang and S. J. Lippard, *Nat. Rev. Drug Discov.*, 2005, **4**, 307-320.
2. L. Kelland, *Nat. Rev. Cancer*, 2007, **7**, 573-584.
3. E. R. Jamieson and S. J. Lippard, *Chem. Rev.*, 1999, **99**, 2467-2498.
4. R. C. Todd and S. J. Lippard, *Metallomics*, 2009, **1**, 280-291.
5. M. D. Hall and T. W. Hambley, *Coord. Chem. Rev.*, 2002, **232**, 49-67.
6. M. D. Hall, H. R. Mellor, R. Callaghan and T. W. Hambley, *J. Med. Chem.*, 2007, **50**, 3403-3411.
7. R. G. Kenny and C. J. Marmion, *Chem Rev*, 2019.
8. S. Marrache, R. Pathak and S. Dhar, *Proc. Natl. Acad. Sci. U.S.A.*, 2014, **111**, 10444-10449.
9. S. Wisnovsky, J. Wilson, R. Radford, M. Pereira, M. Chan, R. Laposa, S. Lippard and S. Kelley, *Chemistry & Biology*, 2013, **20**, 1323-1328.
10. M. Stilgenbauer, A. M. D. S. Jayawardhana, P. Datta, Z. Yue, M. Gray, F. Nielsen, D. J. Bowers, H. Xiao and Y. R. Zheng, *Chem Commun*, 2019, **55**, 6106-6109.
11. Z. Wang, Z. Deng and G. Zhu, *Dalton Trans*, 2019, **48**, 2536-2544.
12. C. C. Konkankit, S. C. Marker, K. M. Knopf and J. J. Wilson, *Dalton Trans.*, 2018, **47**, 9934-9974.
13. D. Gibson, *Dalton Trans.*, 2016, **45**, 12983-12991.
14. T. C. Johnstone, K. Suntharalingam and S. J. Lippard, *Chem Rev*, 2016, **116**, 3436-3486.
15. U. Basu, B. Banik, R. Wen, R. K. Pathak and S. Dhar, *Dalton Trans*, 2016, **45**, 12992-13004.
16. Z. Wang, Z. Xu and G. Zhu, *Angew Chem Int Ed Engl*, 2016, **55**, 15564-15568.
17. J. Mayr, P. Heffeter, D. Groza, L. Galvez, G. Koellensperger, A. Roller, B. Alte, M. Haider, W. Berger, C. R. Kowol and B. K. Keppler, *Chem Sci*, 2017, **8**, 2241-2250.
18. X. Wang, S. Jin, N. Muhammad and Z. Guo, *Chem Rev*, 2019, **119**, 1138-1192.
19. A. Lasorsa, O. Stuchlíková, V. Brabec, G. Natile and F. Arnesano, *Mol Pharm*, 2016, **13**, 3216-3223.
20. Q. Cheng, H. Shi, H. Huang, Z. Cao, J. Wang and Y. Liu, *Chem Commun*, 2015, **51**, 17536-17539.
21. J. Li, S. Q. Yap, C. F. Chin, Q. Tian, S. L. Yoong, G. Pastorin and W. H. Ang, *Chem. Sci.*, 2012, **3**, 2083-2087.
22. I. Tolbatov, C. Coletti, A. Marrone and N. Re, *Inorg Chem*, 2018, **57**, 3411-3419.
23. S. Shamsuddin, C. C. Santillan, J. L. Stark, K. H. Whitmire, Z. H. Siddik and A. R. Khokhar, *J. Inorg. Biochem.*, 1998, **71**, 29-35.
24. T. W. Hambley, A. R. Battle, G. B. Deacon, E. T. Lawrenz, G. D. Fallon, B. M. Gatehouse, L. K. Webster and S. Rainone, *J. Inorg. Biochem.*, 1999, **77**, 3-12.
25. S. R. A. Khan, S. Huang, S. Shamsuddin, S. Inutsuka, K. H. Whitmire, Z. H. Siddik and A. R. Khokhar, *Bioorg. Med. Chem.*, 2000, **8**, 515-521.
26. P. Gramatica, E. Papa, M. Luini, E. Monti, M. B. Gariboldi, M. Ravera, E. Gabano, L. Gaviglio and D. Osella, *J. Biol. Inorg. Chem.*, 2010, **15**, 1157-1169.
27. K. R. Barnes, A. Kutikov and S. J. Lippard, *Chem. Biol.*, 2004, **11**, 557-564.
28. W. H. Ang, I. Khalaila, C. S. Allardyce, L. Juillerat-Jeanneret and P. J. Dyson, *J. Am. Chem. Soc.*, 2005, **127**, 1382-1383.

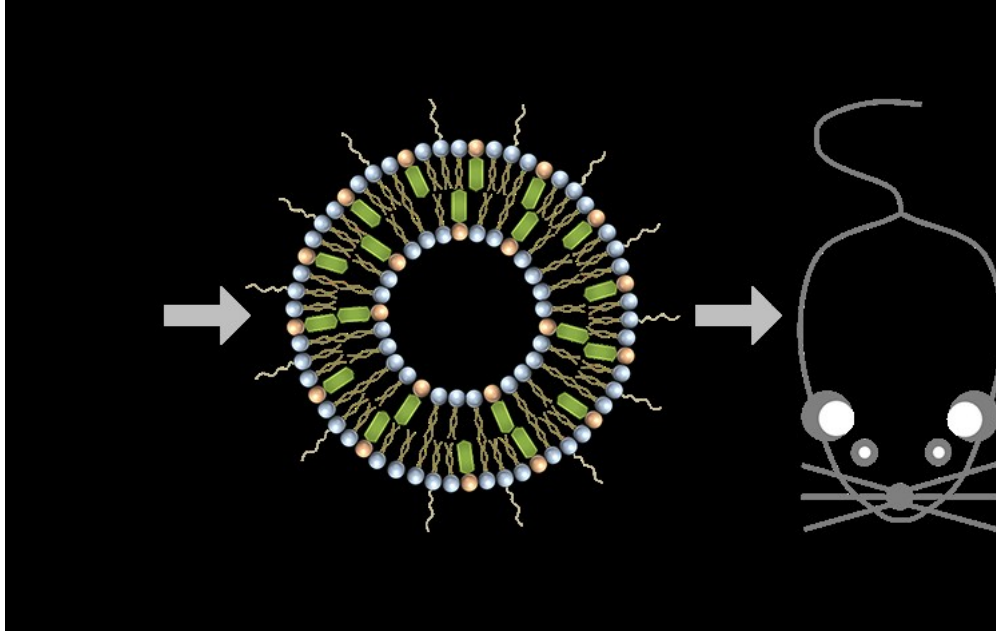
## Journal Name

## ARTICLE

29. S. Dhar and S. J. Lippard, *Proc. Natl. Acad. Sci. U.S.A.*, 2009, **106**, 22199-22204.
30. J. Yang, X. Sun, W. Mao, M. Sui, J. Tang and Y. Shen, *Mol. Pharm.*, 2012, **9**, 2793-2800.
31. K. Suntharalingam, Y. Song and S. J. Lippard, *Chem. Commun.*, 2014, **50**, 2465-2468.
32. S. Dhar, F. X. Gu, R. Langer, O. C. Farokhzad and S. J. Lippard, *Proc. Natl. Acad. Sci. U.S.A.*, 2008, **105**, 17356-17361.
33. S. Dhar, N. Kolishetti, S. J. Lippard and O. C. Farokhzad, *Proc. Natl. Acad. Sci. U.S.A.*, 2011, **108**, 1850-1855.
34. T. C. Johnstone and S. J. Lippard, *Inorg. Chem.*, 2013, **52**, 9915-9920.
35. X. Y. Xu, K. Xie, X. Q. Zhang, E. M. Pridgen, G. Y. Park, D. S. Cui, J. J. Shi, J. Wu, P. W. Kantoff, S. J. Lippard, R. Langer, G. C. Walker and O. C. Farokhzad, *Proc. Natl. Acad. Sci. U.S.A.*, 2013, **110**, 18638-18643.
36. C. He, D. Liu and W. Lin, *Biomaterials*, 2015, **36**, 124-133.
37. H. Xiao, R. Qi, T. Li, S. G. Awuah, Y.-R. Zheng, W. Wei, X. Kang, Song, H., Y. Wang, Y. Yu, M. A. Bird, X. Jing, M. B. Yaffe, M. J. Birrer and P. P. Ghoroghchian, *J. Am. Chem. Soc.*, 2017, **139**, 3033.
38. S. G. Chaney, S. Wyrick and G. K. Till, *Cancer Res*, 1990, **50**, 4539-4545.
39. J. L. Carr, M. D. Tingle and M. J. McKeage, *Cancer Chemother. Pharmacol.*, 2002, **50**, 9-15.
40. Y. Liu, H. Tian, L. Xu, L. Zhou, J. Wang, B. Xu, C. Liu, L. I. Elding and T. Shi, *Int J Mol Sci*, 2019, **20**, E5660
41. C. Garcia-Canton, A. Anadón and C. Meredith, *Toxicol In Vitro*, 2012, **26**, 1075-1086.
42. L. J. Kuo and L. X. Yang, *In Vivo*, 2008, **22**, 305-309.
43. C. A. Brady and L. D. Attardi, *J Cell Sci*, 2010, **123**, 2527-2532.
44. S. G. Awuah, Y.-R. Zheng, P. B. Bruno, M. T. Hemann and S. J. Lippard, *J. Am. Chem. Soc.*, 2015, **137**, 14854.
45. Y.-R. Zheng, K. Suntharalingam, T. C. Johnstone, H. Yoo, W. Lin, J. G. Brooks and S. J. Lippard, *J. Am. Chem. Soc.*, 2014, **136**, 8790-8798.

View Article Online  
DOI: 10.1039/D0DT01297A

Dalton Transactions Accepted Manuscript



63x39mm (300 x 300 DPI)